N72-14872

NATIONAL AERONAUTICS AND SPACE ADMINISTRATION

Technical Memorandum 33-515

Temperature Control of the Mariner Mars 1971 Spacecraft

Larry N. Dumas

JET PROPULSION LABORATORY
CALIFORNIA INSTITUTE OF TECHNOLOGY
PASADENA, CALIFORNIA

January 1, 1972

NATIONAL AERONAUTICS AND SPACE ADMINISTRATION

Technical Memorandum 33-515

Temperature Control of the Mariner Mars 1971 Spacecraft

Larry N. Dumas

JET PROPULSION LABORATORY
CALIFORNIA INSTITUTE OF TECHNOLOGY
PASADENA, CALIFORNIA

January 1, 1972

PREFACE

The work described in this report was performed by the technical divisions of the Jet Propulsion Laboratory, under the cognizance of the Mariner Mars 1971 Project.

ACKNOWLEDGMENT

This report was compiled by L. N. Dumas using data from many sources. J. A. Hultberg, W. A. McMahon, H. L. Nordwall, and L. D. Stimpson were responsible for the spacecraft thermal design and analysis; R. A. Becker planned and directed the thermal test program, and H. D. von Delden designed and supervised the construction of the subsystem thermal shielding.

CONTENTS

I. Introduction 1

II. System Thermal Design and Development 3

A. Design Description 3

B. Analysis 5

C. System Level Tests 6

III. Subsystem Design and Development 9

A. Design Description 9

B. Hardware Developmental Efforts 11

C. Blanket Fabrication Techniques 13

D. Developmental, Verification and Qualification Tests for Hardware 14

E. Blanket Emittance Tests 14

IV. Flight Results 17

V. Conclusions and Recommendations 18

References 20

TABLES

1. Spacecraft temperature control requirements 21

2. Spacecraft bus comparisons 23

3. Comparison of test temperatures with analytical predictions 24

4. Test/analysis comparison summary 25

5. Test and flight temperatures 26

6. Temperature control subsystem equipment list 28

7. Results of propulsion module effective emittance tests . . . 29

8. Mariner 9 earth cruise temperatures, Day 155 GMT 30

CONTENTS (contd)

FIGURES

1. Average bus temperature vs power 31

2. Scan platform temperature distribution 32

3. Mariner Mars 1971 spacecraft, top view, Bay VIII side . . . 33

4. Mariner Mars 1971 spacecraft, bottom view, Bay II side . . 34

5. Propulsion module mold 35

ABSTRACT

The Mariner Mars 1971 orbiter mission was a part of the ongoing program of unmanned planetary exploration. The spacecraft design was based on that of Mariner Mars 1969, with changes as necessary to achieve mission objectives. The thermal design for Mariner Mars 1971 is described herein, with emphasis on those areas in which significant changes were implemented. Developmental tasks are summarized and discussed, and initial flight data are presented.

I. INTRODUCTION

The objective of the Mariner Mars 1971 mission was to study the characteristics of the planet from a Mars orbit for a period of at least 90 days. Mariner 9, the second of the flight spacecraft, was successfully launched on a trajectory to Mars on May 30, 1971; orbit insertion was achieved on November 14, 1971, GMT. It was planned that about 70% of the planet's surface would be mapped during the first 90 days in orbit. The characteristics of the atmosphere and Martian surface were to be studied, and data on variations in surface markings over the mission lifetime were to be obtained. The scientific payload included two television cameras, ultraviolet and infrared spectrometers, and an infrared radiometer.

The spacecraft design was based on that of Mariner Mars 1969, with modifications only as required to meet mission objectives. The most significant changes thermally were (1) the addition of a 1334-N (300-lb) thrust rocket and associated propulsion subsystem for orbit insertion, (2) the switch from a silver-zinc to a nickel-cadmium battery with resultant changes in power conditioning equipment, (3) the change to an interferometer-type infrared spectrometer, and (4) configuration changes necessary to accommodate these changes and other mission requirements. The Mariner Mars 1969 spacecraft design is described in detail in Refs. 1 and 2; the corresponding description for Mariner Mars 1971 is contained in Ref. 3.

Previous missions to Mars in 1964 (Mariner 4) and 1969 (Mariners 6 and 7) were completely successful in terms of temperature control. The thermal design approach for MM'71 drew heavily on this experience, and some of the residual hardware from MM'69 was used for MM'71. The spacecraft changes from MM'69 were thermally significant, however, and the scope of the developmental effort in temperature control was comparable to that of MM'69.

Key milestones in the MM'71 project from the temperature control viewpoint were:

1968

May 21	Inputs to feasibility study submitted
September 1	Project authorization document issued
October 1	Science payload selected

1969

February 21	Spacecraft system functional design review
March 21	Temperature control subsystem functional design review
June 20	Spacecraft system detail design review
July 17	Temperature control subsystem detail design review

1970

March 17	Temperature control model (TCM) simulator test completed
August 8	Proof test model (PTM) simulator test completed
December 19	M'71-1 simulator test completed
January 18	M'71-2 simulator test completed

1971

February	PTM delivered to AFETR
March	M'71-1 and M'71-2 delivered to AFETR
May 8	M'71-1 (Mariner 8) launched
May 30	M'71-2 (Mariner 9) launched

II. SYSTEM THERMAL DESIGN AND DEVELOPMENT

A. Design Description

The MM'71 thermal design was generally similar to MM'69, which is described in Ref. 4. Further descriptions of typical Mariner designs are contained in Refs. 5-8. Details of the MM'71 design are given in Ref. 9, and design criteria and functional requirements are given in JPL MM'71 Functional Requirements Documents M71-3-210 and M71-4-2011 (Ref. 1). Table 1 summarizes the thermal design requirements. For purposes of description the spacecraft can be subdivided into four more or less thermally separable zones: bus, propulsion module, scan platform, and appendages.

1. Bus (main equipment compartment). The basic thermal design for the Mariner bus has proven to be flexible, reliable, and durable. Mariner Mars 1971 was the fourth spacecraft series to use the basic insulated sandwich approach, in which the upper and lower surfaces of the octagon were insulated and most of the dissipated electronics power was rejected through thermostatically controlled variable emittance louvers mounted on the electronic bay faces. The result was a forgiving design, insensitive to the changes and uncertainties in thermally significant parameters which are characteristic of flight projects. A gross comparison of the 1971 bus with those of past Mariner spacecraft is given in Table 2. In addition to the obvious differences noted in Table 2, the nonlouvered emittance-area product and the solar heating input contributed to the specific thermal characteristics of each design.

Figure 1 shows the average bus temperature vs heat dissipation for the combined bus and propulsion module enclosure for the M'71-1 spacecraft derived from space simulator test results; PTM and M'71-2 characteristics were essentially identical to these. Additional data on the thermal design characteristics are given in Ref. 10.

2. Propulsion module. The basic design approach for the propulsion module was to superinsulate the module exterior and thermally couple the module to the maximum extent possible with the thermostatically controlled bus. During TCM testing, when heat transfer across the tank

interiors was intentionally prevented, the temperature of the thrust plate structure bridging the tank tops was found to follow the simple equation

$$1.03(T_P - T_B) + 455\sigma T_P^4 - 185S - P = 0$$

where

T_P = thrust plate temperature, °K

T_B = average bus temperature, °K

S = solar intensity, W/cm^2

P = thrust plate heater power, W

Flight data indicated that the heat path through the propellants may have significantly improved the bus-propulsion module coupling (see Section IV). A 10-W commandable heater was attached to the thrust plate for use at lower solar intensities to reduce in-flight temperature variations.

Cruise temperature control for the rocket engine was achieved by radiatively coupling the valve end of the engine with the propulsion module interior. The engine nozzle extended outside the blanketed module, and high-temperature shields and blankets were provided to protect the module from engine skirt radiation during firing. Alignment of the engine axis along the sun line created a potential problem of focusing sunlight into the combustion chamber with resultant overheating of the valve and excessive solar inputs to the tank tops. The L605 skirt was grit-blasted to eliminate any specularity which would contribute to this condition. At earth solar intensity, about 11.3 W of the 50 W entering the exit plane ultimately reached the combustion chamber.

3. Scan platform. The thermal design for the platform followed closely that of MM'69. The only significant payload change was the substitution of the infrared interferometer spectrometer (IRIS) for the infrared spectrometer (IRS). All instruments except the IRIS optics were thermally coupled inside a blanketed enclosure, with a modest degree of thermostatic control provided by a half-set of louvers mounted to the ultraviolet spectrometer (UVS).

The replacement heaters in each platform instrument were powered directly off the DC bus in order to minimize power conversion inefficiencies and conserve 2.4-kHz power. As a result, platform cruise temperatures varied as solar panel voltages changed in flight. This effect, as well as platform temperature sensitivity to power, can be seen in Fig. 2. Figure 2 gives composite data for the two flight spacecraft and the PTM. It should be noted that platform temperatures were higher for the MM'71 spacecraft than for MM'69. The IRIS optics were thermostatically controlled at 250°K (-10°F) with an on-off heater (~12 W max at Mars). The thermal design for this portion of the instrument, which was thermally isolated from the base, was the responsibility of Texas Instruments, Inc.; JPL provided boundary condition data to Texas Instruments.

4. Appendages. The temperature control for external appendages was passive, relying primarily on thermal-optical property and conduction path control to achieve desired temperatures. Items in this category included acquisition and cruise sun sensor assemblies, attitude control gas jet assemblies, solar panels, panel cruise dampers, and the three S-band antennas. Perhaps the most significant new problem in this area was posed by the cruise sun sensor/sun gate assembly, which was situated on the Bay III outrigger. On previous Mariner spacecraft this assembly had been conductively tied to the bus. On MM'71, the assembly was conductively isolated from the outrigger and a continuous 1.5-W DC heater was added to help suppress the earth-to-Mars temperature change.

B. Analysis

The spacecraft bus and scan platform computer model was programmed for the Univac 1108, using the Chrysler Improved Numerical Differencing Analyzer (CINDA) general-purpose heat-transfer program. It consisted of 330 nodes; part of the scan platform model of 250 nodes was originally developed for the MM'69 spacecraft. Steady-state analysis of the propulsion module was performed on the Thermal Analyzer System (TAS) on the 1108, and transients were run using CINDA. The propulsion module analyses ranged up to 75 nodes, but the final model contained only 12. All models were updated after the TCM test and again after the flight spacecraft tests.

These models were used both for design and prediction of flight temperatures for untested modes, such as launch, midcourse maneuver, and orbital transients.

Some insight into the accuracy of the analytical modeling of the spacecraft thermal characteristics can be obtained by comparing pretest predictions with actual temperatures observed during the temperature control model (TCM) and proof test model (PTM) space simulator tests. The former test provided the first opportunity for checking and upgrading the analytical model; the latter test provided the first such opportunity with a flight-type spacecraft. These comparisons are therefore most meaningful in establishing the accuracy of the analyses prior to model modifications based on the test data. Table 3 presents this comparison for representative spacecraft locations for the TCM and PTM. The test modes listed for these two spacecraft are not directly comparable, but the test data and analytical predictions for each mode do correspond. Table 4 summarizes the results from Table 3 by listing the number of test-to-analysis differences which fell within the 2.8°C (5°F) bands given. It is probably fair to characterize the main sources of error for the TCM test as inaccuracies in modeling the spacecraft physical characteristics, while the PTM errors were mostly caused by poor estimates of power dissipation. In this regard, notice that the actual PTM temperatures were typically lower than the predictions, indicating that power estimates were usually high.

C. System Level Tests

1. Temperature control model. The TCM was a full-scale mockup of the flight spacecraft, with particular attention given to duplication of significant thermal paths (conductive and radiative), external configuration, and surface thermal radiative properties. Electronic power dissipation was simulated with rheostat-controlled resistance heaters.

The TCM test was conducted in March 1970, over a two-week period. Although minor thermal design iterations continued into the flight spacecraft test period, for practical purposes the end of the TCM test also marked the end of the detail design and development period. At the same time, this

test was the first milestone in the verification cycle for the system level thermal design. Primary thermal test objectives were to:

(1) Verify that the thermal design was adequate, reliable, and flexible.

(2) Evaluate empirically the thermal characteristics of the design.

(3) Obtain good vacuum data on the effects of a simulated engine firing.

The results of the TCM test indicated that minor modifications to the baseline thermal design were sufficient to insure that all temperatures would remain within desirable limits throughout the mission. The design was found to be reliable and flexible enough to accommodate both power and test uncertainties. A sufficient number of modes were simulated not only to verify the design but to determine all of the major coupling factors and solar/power sensitivities of importance. Descriptions of the TCM and of the test are given in detail in Ref. 11.

2. <u>Verification, qualification, and flight acceptance tests.</u> The space simulator testing of the proof test model from July 26 to August 8, 1970, constituted both the actual and formal thermal design verification and flight qualification. Flight acceptance space simulator testing of M'71-1 was performed December 12 to 19, 1970, and similar tests on M'71-2 were performed January 12 to 20, 1971.

The primary objectives of the PTM test from the temperature control point of view were to:

(1) Verify the capability of the thermal design to maintain acceptable temperatures under flight conditions of environment and operating modes.

(2) Identify design modifications to enhance thermal performance.

(3) Obtain correlation with TCM results to make TCM data applicable to flight-type spacecraft.

(4) Obtain more detailed information on thermal characteristics of design to assist in temperature predictions needed for flight operations.

(5) Obtain Phase I and II correlation to correct certain Phase I data and to assist in the evaluation of the necessary test configuration for flight spacecraft.

The primary objectives of the flight spacecraft tests from the temperature control point of view were to:

(1) Verify the capability of the thermal design features and flight temperature control hardware to maintain acceptable temperatures under flight conditions of environment and operating modes.

(2) Verify the adequacy of thermal design modifications implemented on the basis of PTM test results.

(3) Obtain comparison of thermal characteristics of flight-type spacecraft.

(4) Obtain information on thermal characteristics of each flight spacecraft to provide a basis for temperature predictions needed for mission operations.

From the test results it was concluded that the temperature control design would successfully maintain all temperatures within allowable limits, although certain design changes were indicated to provide additional margin or optimize operating conditions. The test data agreed reasonably well with pretest predictions. A complete test summary can be found in Ref. 10.

Table 5 summarizes significant test data and provides a comparison of this data with flight results and with the target temperature ranges.

III. SUBSYSTEM DESIGN AND DEVELOPMENT

A. Design Description

The Mariner 1971 temperature control subsystem included superinsulation blankets, rigid metallic shields, and variable emittance louvers. Seventy separate items were delivered to the spacecraft assembly facility (SAF), including 6 thermal blankets, 17 polished aluminum shields, 6 louver assemblies, 4 rocket motor shields, and various support and attachment hardware (excluding fasteners). The approximate total area covered by blankets, shields, and louvers was 12.1 m^2 (130 ft^2) compared to 6.9 m^2 (75 ft^2) for MM'69. Table 6 gives a subsystem weight summary.

Figures 3 and 4 show the major hardware elements comprising the temperature control subsystem. A brief description of these elements is given below.

1. <u>Variable emittance louvers.</u> The six louver assemblies on the bus and the half-set on the scan platform were identical to their MM'69 counterparts. In fact, the hardware used was residual MM'69 equipment. Incipient opening temperature was 13°C (55°F) for the louvers on Bays I, II, III, V, and VII, 4°C (40°F) for Bay VIII, and -18°C (0°F) for the scan platform. The effective emittance varied from approximately 0.1 to 0.7 over a 17°C (30°F) actuation range. The same basic louver design has been used on all Mariner spacecraft since MM'64, and the design features are well documented (see especially Ref. 12).

2. <u>Upper (propulsion module) thermal blanket.</u> The size and configuration of the propulsion module required a complete departure from the upper blanket design of MM'69. The new blanket had an area of 6.6 m^2 (71 ft^2) and weighed 5 kg (11 lb) as compared to 1.8 m^2 (19 ft^2) and 0.95 kg (2.1 lb) for MM'69.

The new blanket design provided micrometeoroid protection by the addition of a Teflon-coated glass cloth (Dupont Armalon 95049) outer layer. Fifteen layers of 0.0038-mm (1/8-mil) Mylar, aluminized on both sides, were used. These layers were separated with Nylon net; each Mylar layer was perforated (for venting) to 1% open area. The required three-dimensional contours were achieved using a random-pattern tape-up of the Mylar and net

over a special mold, a process which is described below in greater detail. A Dacron "filter" layer was provided on the vented (inner side) of this shielding to prevent any loose particles in the blanket from escaping. The inside of the resultant blanket was faced with 0.025-mm (1-mil) FEP Teflon, aluminized on the side facing the blanket. There were no through seams or joints; the closure was overlapped and secured with an ordinary shoestring-type lace and tie. The lower edge of the blanket was secured with a drawstring.

3. Lower thermal blanket. This blanket had only minor modifications from the MM'69 design. The octagonal layup had 10 pairs of Mylar and net and was fabricated from a flat pattern. The facing layers were the same as for the upper blanket, except the Armalon was replaced with 0.025-mm (1-mil) Teflon.

4. Scan platform blanket. This blanket was fabricated on a mold in the same manner as the upper blanket. The layup was the same as the lower blanket, except that 8 pairs of Mylar and net were used instead of 10. The complex configuration of the blanket required four lace joints, two drawstrings, and two restraining tie points for installation.

5. Rocket engine shielding. The thermal shield was divided into two parts, the metal thermal shield assembly and the rocket engine multilayer thermal blanket. These assemblies protected sensitive components from radiation from the engine nozzle during firing. The shield protected the gimbal ring and actuators, and the Kapton blanket protected the propulsion module blanket.

The shield installation included a 31.8-cm (12.50-in.) diameter gold-plated titanium assembly, four titanium standoffs and a cylindrical aluminum assembly. The 61-cm (24-in.) diameter blanket was 10 layers of gold-coated 0.013-mm (1/2-mil) Kapton with an aluminized 0.051-mm (2-mil) Kapton cover sheet.

6. IRIS shield and shade. Although the base of the instrument was enclosed by the scan platform blanket, the optics portion required thermal blanket insulation. Mockup instruments were supplied to JPL for the design and fabrication of flight blankets. A flat pattern construction was developed to fabricate a 15-layer Mylar MM'71-type blanket, with the inner and outer

layers of 0.025-mm (1-mil) aluminized Teflon. The blanket was secured to the instrument by a drawstring around the base. The flight blankets fabricated by JPL were delivered to TI for installation on the instrument prior to SAF delivery.

A deployable shade to block thermal radiation from the planet which would otherwise impinge on the optics primary radiating surfaces was installed on the Mars side of the instrument. The shade assembly was constructed of a single sheet of 0.127-mm (5-mil) Mylar aluminized on one side. The deployment and support of the shade was accomplished by a 0.635-mm-diam (0.025-in.) music wire frame that was taped and tied to the Mylar. In the stowed position the shade was flexed to a curved configuration to permit contact with a deployment guide on the adapter, which provided a smooth surface for the shade to slide against when the spacecraft separated from the adapter.

7. Polished aluminum shields. Areas around the louvers and one bay of the bus were shielded by polished aluminum covers. There were 17 such shields used on MM'71, and eight of those were identical to MM'69. The thermal and structural design of the shields was similar to those of Mariners 1964, 1967, and 1969.

B. Hardware Developmental Efforts

During the MM'71 developmental cycle a number of new design problems were faced and certain design improvements were implemented. The more significant of these are summarized below.

1. Multilayer insulation separator selection. After considering various types of separators, including the MM'69-type Nylon net, a new type of Nylon net was selected for MM'71 because of low weight, ease of fabrication, good thermal performance, low outgassing and low cost. The D. Strauss & Co. style 11000 Nylon net was special-ordered without dye coloring, fire proofing or the mildew-resistant coating. A sample blanket was fabricated using this Nylon net separator to determine the layup density and mechanical properties. A comparison of this layup with a MM'69 type showed a weight saving of approximately 0.59 kg (1.3 lb) on the 6.6-m^2 (71-ft^2) propulsion module blanket. This was a significant improvement, since the Mylar and net were only 29% of the total weight of 5 kg (11 lb). The MM'71

blanket design was judged to be superior, as was eventually proven by the propulsion module blanket evaluation test and calorimeter tests.

2. Blanket filter layer. The innovation of a filter layer for MM'71 was the result of efforts to eliminate particulate contamination of the spacecraft. During the construction of a thermal blanket, the cutting of the Mylar and net produced small slivers and particles of Nylon filament. A 2.5-cm (1-in.) long cut of the net could produce as many as 360 pieces of Nylon, 0.02-mm (0.0008-in.) diam by approximately 0.76 mm (0.030-in.) long. These particles could escape from the blanket during the decompression phase through the holes provided for venting. Several candidate filter materials were considered, including Nylon and Teflon millipore-type and nonwoven fabrics; fitting individual vents with filters as opposed to the one continuous filter layer was also considered. The Dacron fabric selected was a J. P. Stevens & Co. 113 × 80, 70 denier plain weave that weighed 66.5 g/m^2 (1.96 oz/yd^2).

3. Micrometeoroid protection. In a separate investigation of micrometeoroid barriers, a Teflon-coated glass cloth processed by E. I. DuPont designated Armalon 95049 was selected. This material had been previously qualified for the Apollo program by NASA MSC, Houston. This white fabric was approximately 0.2 mm (0.008 in.) thick and weighed 25.52 g/m^2. A single layer covering the MM'71 propulsion module gave the protection required. Rather than providing this layer as a separate item, it was incorporated as the outside layer of the propulsion module thermal blanket in place of the usual 0.025-cm (1-mil) Teflon. The Armalon provided a rugged outside layer and had no effect on blanket thermal performance.

4. Electrostatic problem. During the handling and installation of the TCM propulsion module blanket, a potentially hazardous electrostatic charge buildup was noted. The three potential problem areas were (1) the discharge of pyrotechnic devices, (2) damage to sensitive electronic components, and (3) personnel discomfort resulting in additional risk of inadvertent spacecraft damage.

The materials involved were the Dacron filter layer, the Armalon outside layer, and Kapton film used on the rocket engine thermal blanket. These materials were tested separately by the PAA environmental health

laboratory at Kennedy Space Center, Florida. The result of that testing showed induced electrostatic potentials of up to 20,000 V with a bleedoff time of 5 min. At JPL, potentials of 100,000 V were measured with a CMI 7777 static meter under uncontrolled conditions.

After investigation of the phenomenon and consideration of various solutions, the following steps were taken: (1) one side of the Armalon and the Kapton was metallized, and (2) a 0.025-cm (1-mil) metallized Teflon inside layer with the metal side toward the Dacron filter layer was added. Any local charge on the dielectric induced an equal and opposite charge on the conductor, which effectively canceled the external field ("grounding" of the conductor occurred via ionization in the air). The aluminized Armalon and Kapton were again tested for electrostatic potential as was a sample of the thermal blanket assembly. No potential could be induced in the separate materials, and the blanket produced only a -1000-V potential when rubbed with wool. The results were considered successful and the modifications were made to the flight blankets.

C. Blanket Fabrication Techniques

The MM'69 planetary scan platform was the first Mariner equipment to require a seamless, contoured blanket to achieve necessary thermal properties while satisfying configuration requirements. The fabrication techniques developed for this application were extended and improved to meet the requirement for a highly efficient blanket for the MM'71 propulsion module. The essence of the technique was to lay-up the blanket on a configuration model in such a way that the taped joints were not aligned on successive layers. The resultant "seamless" blanket was thermally superior to the usual flat pattern types, which have a number of seams and joints that penetrate the blanket and degrade its performance.

The key to the successful use of this technique was the fabrication of the configuration models, or molds, for the scan platform and propulsion module. These molds supported the blankets during fabrication and provided all necessary dimensional data. It should be noted that engineering drawings of the blankets built in this way contained only assembly and material details; no attempt was made to commit the complex geometries to paper.

The construction of the propulsion module mold will be described to illustrate the process. The mold was constructed over a mockup which contained the hardware defining the necessary blanket configuration. The mockup was covered with aluminum screen to serve as a base for plastering. Care was taken in the screening to keep the screen below the anticipated finished plane of the mold. The first thin coat of pottery casting plaster was then applied to the screen to form a rigid shell. The finished planes were established by additional plaster, up to 15 cm (6 in.) thick, and contoured by scrapers to a smooth finish. The completed mold was complex in shape; all planes were carefully developed with consideration given to the capability of the multilayer thermal blanket to conform to the configuration. A series of magnets were imbedded in the plaster mold to retain sheet metal forms which were placed on top of the Mylar and net layers as the fabrication progressed. Figure 5 shows the finished mold with a paper cover which was being used to determine the Armalon yardage requirements. The black lines are the minimum seams required to closely fit a flat surface to the propulsion module and show why a seamless construction was considered necessary.

D. Developmental, Verification and Qualification Tests for Hardware

The various tests performed on the thermal hardware are covered in some detail in Ref. 13. The propulsion module thermal blanket evaluation tests were such a critical element in the overall thermal design evolution that a brief summary is given below.

E. Blanket Emittance Tests

The test fixture for the emittance tests consisted of an aluminum skeleton structure which provided the proper configuration at all of the points where the thermal blanket came in contact with the propulsion module. A guard-heated octagonal aluminum plate served as an adiabatic bottom closure. Heat applied in the interior of the blanket cavity was thus rejected only through the blanket.

The blanket configuration for the first seven modes consisted of different combinations of various blanket components as described in Table 7. In each configuration there were no penetrations through the

blanket except where it interfaced with the baseplate. These modes were selected to investigate the following areas of interest:

(1) The relationship between number of layers and effective emittance (Modes 1, 3, 4 and 6).

(2) The effect of a low-emittance outer layer on effective emittance (Mode 2 vs Mode 1).

(3) Reproducibility of blanket construction (Mode 5 vs Mode 1).

(4) Comparison of MM'69 Materials and fabrication techniques with those proposed for MM'71 (Mode 7 vs Mode 1).

The blanket tested in Mode 3 (Dacron inner layer, 15 0.0038-mm 1/8-mil Mylar/MM'71 net layers, and an Armalon outer layer) was selected as the flight blanket for the following reasons:

(1) The 14% decrease in ϵ_{eff} (2.5 W) afforded by the 20-layer blanket over the 15-layer blanket was not considered sufficient to warrant the extra weight and fabrication time.

(2) The Mariner Mars 1969 type blanket was eliminated because of its additional weight (10%) and the fact that it was somewhat more difficult to fabricate.

(3) The low-emittance outer layer used in Mode 2 provided a substantial (16%) decrease in effective emittance over the high-emittance (Armalon) outer layer, but the Mylar outer layer used on Mode 2 would have severely overheated when subjected to solar irradiation. Medium emittance compromises would not have improved blanket performance enough to justify the developmental effort and special handling required.

Once the flight blanket was selected, the 30 layers of Mylar and net were sewn to the Dacron and Armalon, and the rocket engine and omniantenna cutouts were made. All flightlike seams were incorporated and the flightlike closure (i.e., lacing) was made at the blanket opening along the outboard side of the omniantenna instead of the simple taped overlap used for the first seven modes. The engine and omniholes were then covered with

0.051-mm (2-mil) aluminized Kapton (aluminum side out), and the blanket was tested at two different temperature levels (Modes 8 and 9). The results indicated that the total seam effect was an increase of 20% in effective emittance (or 2.3 W). Later calorimeter tests of samples of the blanket selected yielded effective emittances in the range from 0.002 to 0.003, indicating that factors unique to the fabrication had a controlling effect on the flight blanket effectiveness.

IV. FLIGHT RESULTS

Flight temperature predictions for cruise were made prior to launch on the basis of corrected simulator data. Table 8 compares these predictions with the flight data for Mariner 9 after temperature stabilization. The large errors in TWT base temperature were caused by a switch in the on-line TWT; when this effect is taken into account, the actual differences were less than 2°C (4°F). The only other difference of any significance was the sun sensor/sun gate temperature, which was 4.4°C (8°F) above prediction. This assembly was operating at its upper limit of 49°C (120°F) near earth, which caused some concern. It appears that the discrepancy was mainly due to incorrect interpretation of test data.

The behavior of the propulsion module temperatures during the first days of flight was somewhat anomalous, though not alarming. The temperature of the fuel and oxidizer tanks prior to tank pressurization was 3°C (6°F) below the prelaunch predicted values. After tank pressurization, both propellant tanks increased 1°C (2°F) and were stable at 2°C (4°F) below the predicted temperatures. Both tanks dropped 1°C (2°F) immediately after engine firing due to gas expansion in the tanks. Subsequently, the fuel tank increased 1°C (2°F) and stabilized 2°C (4°F) below the predicted temperature of 23°C (73°F). The oxidizer tank increased 2°C (4°F) after the maneuver and stabilized only 1°C (2°F) below the predicted temperature of 22°C (71°F). The effect of the propulsion heater turn-on was 5°C (9°F) at the tank tops, as compared with a preflight prediction of 7°C (12°F).

The flight temperature history noted above suggests that the internal heat transfer characteristics of the tanks changed with time in such a way that the thermal coupling between the engine and bus ends of the tanks decreased. A probable explanation for the initial difference between predicted and actual temperatures is that this coupling was larger than expected. It appears possible that some form of (variable) mass transfer occurred in the propellants due to surface tension effects or attitude control limit cycling.

V. CONCLUSIONS AND RECOMMENDATIONS

1. The MM'71 thermal design and temperature control subsystem hardware provided acceptable flight temperatures, demonstrating the adequacy of the design features and the implementation thereof.

2. The reduced space simulator test program for MM'71 created a requirement for maximizing the integration of thermal test objectives with spacecraft functional verification. This requirement was satisfied by close cooperation of the system test directors and the temperature control engineers in both the planning and execution of the test.

3. The nature of the mission and the reduced test program for MM'71 tended to increase the reliance on analysis and decrease the reliance on test, as compared with past Mariner temperature control efforts. The effect of this shift in emphasis was not harmful, although the cost reduction implemented through reduction in testing undeniably carried some element of risk. It is this cost vs risk tradeoff which is at the heart of the decision with respect to the analysis vs test tradeoff. Some progress was made on MM'71 toward decreasing cost without unduly increasing risk.

4. The definition of temperature limits can be affected by the following considerations:

Criterion	Responsibility
Equipment design requirements	System engineer
Equipment survival and operating characteristics	Design agency
Temperature control capabilities	Temperature control engineer
Qualification and acceptance test levels	Environmental requirements engineer

Some confusion and misunderstanding as to the interrelationship of these criteria existed on MM'71, underscoring the need for adequate communications between affected parties.

5. The fact that temperature control was implemented both by subsystem and system design features and by specialized hardware and the fact that the design was finalized at a relatively late date led to some concern that the

early progress of the design was inadequate. The successful completion of the thermal development indicates that these concerns were not well founded, but temperature controllers on future projects would do well to insure that the nature of the temperature control process is understood by affected project elements.

REFERENCES

1. Mariner Mars 1969 Spacecraft Design Book, JPL internal document. Jet Propulsion Laboratory, Pasadena, Calif.

2. Mariner Mars 1969 Final Project Report, Technical Report 32-1460, Vol. I, Jet Propulsion Laboratory, Pasadena, Calif., Nov. 1, 1970.

3. Mariner Mars 1971 Orbiter Spacecraft Design Book, JPL internal document. Jet Propulsion Laboratory, Pasadena, Calif.

4. Flight Projects, Space Programs Summary 37-55, Vol. I, pp. 5-18. Jet Propulsion Laboratory, Pasadena, Calif., Jan. 31, 1969.

5. Dumas, L. N., Temperature Control of the Mariner Venus 67 Spacecraft, Technical Report 32-1284, Jet Propulsion Laboratory, Pasadena, Calif., July 15, 1968.

6. Lewis, D. W., Miller, D. C., and Dumas, L. N., Mariner Mars 1964 Temperature Control Subsystem, Technical Report 32-957. Jet Propulsion Laboratory, Pasadena, Calif., Sept. 15, 1967.

7. Schmuecker, J. D., "Engineering Mechanics Division Historical Summary – Mariner Venus 67," Internal Document 604-37. Jet Propulsion Laboratory, Pasadena, Calif., Mar. 1, 1968.

8. Lewis, D. W., "Engineering Mechanics Division Historical Summary – Mariner Mars 1969," Internal Document 605-238. Jet Propulsion Laboratory, Pasadena, Calif., Aug. 17, 1970.

9. Flight Projects, Space Programs Summary 37-57, Vol. I, pp. 56-58. Jet Propulsion Laboratory, Pasadena, Calif., May 31, 1969.

10. Becker, R., Hultberg, J., Nordwall, H., and Stimpson, L., "Mariner Mars 1971 PTM and Flight Spacecraft Space Simulator Tests Temperature Control Report," Internal Document 610-177. Jet Propulsion Laboratory, Pasadena, Calif., June 15, 1971.

11. Becker, R. A., "Mariner Mars 1971 Temperature Control-Model Test Report," Internal Document 610-150, Jet Propulsion Laboratory, Pasadena, Calif., Jan. 1971.

12. Carroll, W., Coyle, G. G., and von Delden, H., Mariner Mars 1964 Temperature Control Hardware Design and Development, Technical Report 32-955. Jet Propulsion Laboratory, Pasadena, Calif., June 1, 1967.

13. Schmuecker, J. D., "Engineering Mechanics Division Historical Summary – Mariner Mars 1971," Internal Document 610-166. Jet Propulsion Laboratory, Pasadena, Calif., to be published.

Table 1. Spacecraft temperature control requirements

Assembly	Operating range, °C(°F)			Nonoperating range, °C(°F)			Maximum acceptable temperature during ground operations (in air), °C(°F)
	Allowable long-term range (>1 h)	Allowable short-term range (<1 h)	Preferred range	Allowable long-term range (>1 h)	Allowable short-term range (<1 h)	Preferred range	
Bus							
Bay I (power)	10 to 40 (50 to 104)	5 to 50 (41 to 122)	10 to 32 (50 to 90)	0 to 50 (32 to 122)	0 to 55 (32 to 131)	10 to 32 (50 to 90)	55 (131)
Bay II (power IRIS and SCAN)	10 to 40 (50 to 104)	5 to 50 (41 to 122)	14 to 37 (58 to 98)	0 to 50 (32 to 122)	0 to 55 (32 to 131)	10 to 32 (50 to 90)	55(131)
Bay III (CC and S and AC Electronics)	13 to 43 (55 to 110)	13 to 43 (55 to 110)	18 to 35 (65 to 95)	13 to 43 (55 to 110)	0 to 43 (32 to 110)	16 to 43 (60 to 110)	43(110)
Bay IV (FCS and FTS)	5 to 40 (41 to 104)	5 to 50 (41 to 122)	10 to 32 (50 to 90)	0 to 50 (32 to 122)	0 to 55 (32 to 131)	10 to 32 (50 to 90)	55(131)
Bay V (DSS)	10 to 50 (50 to 122)	5 to 50 (41 to 122)	10 to 32 (50 to 90)	0 to 50 (32 to 122)	0 to 50 (32 to 122)	10 to 32 (50 to 90)	50(122)
Bay VI (RFS)	5 to 50 (41 to 122)	5 to 50 (41 to 122)	10 to 32 (50 to 90)	0 to 50 (32 to 122)	0 to 55 (32 to 131)	10 to 32 (50 to 90)	55(131)
Bay VII (DAS and TV)[a]	5 to 50 (41 to 122)	5 to 50 (41 to 122)	10 to 32 (50 to 90)	0 to 50 (32 to 122)	0 to 55 (32 to 131)	10 to 32 (50 to 90)	55(131)
Bay VIII (battery)	-1 to 32 (30 to 90)	-1 to 38 (30 to 100)	10 to 18 (50 to 65)	-1 to 32 (30 to 90)	-7 to 49 (20 to 120)	10 to 27 (50 to 80)	49(120)
Canopus sensor	-7 to 38 (20 to 100)	-7 to 46 (20 to 115)	4 to 27 (40 to 80)	-7 to 38 (20 to 100)	-7 to 46 (20 to 115)	4 to 27 (40 to 80)	38(100)
AC nitrogen tanks	5 to 50 (41 to 122)	0 to 55 (32 to 131)	10 to 32 (50 to 90)	0 to 55 (32 to 131)	0 to 55 (32 to 131)	10 to 32 (50 to 90)	55(131)
Scan actuator (clock)	5 to 50 (41 to 122)	0 to 55 (32 to 131)	5 to 50 (41 to 122)	0 to 55 (32 to 131)	0 to 55 (32 to 131)	0 to 55 (32 to 131)	55(131)
Pyro electronics	0 to 55 (32 to 131)	0 to 55 (32 to 131)	10 to 32 (50 to 90)	0 to 55 (32 to 131)	0 to 55 (32 to 131)	10 to 32 (50 to 90)	55(131)
Platform							
Scan actuator (cone)	-25 to 30 (-13 to 86)	-25 to 30 (-13 to 95)	-18 to 30 (0 to 86)	-25 to 30 (-13 to 86)	-30 to 35 (-22 to 95)	-18 to 30 (0 to 86)	55(131)
IRIS optics[b]	-26 to -21 (-14 to -5)	-26 to -21 (-14 to -5)	-26 to -21 (-14 to -5)	-26 to -21 (-14 to -5)	-26 to -21 (-14 to -5)	-26 to -21 (-14 to -5)	35(95)
IRIS electronics	-3 to 27 (27 to 80)	-5 to 40 (23 to 104)	-3 to 27 (27 to 80)	-3 to 27 (27 to 80)	-5 to 40 (23 to 104)	-3 to 27 (27 to 80)	40(104)
TV-A vidicon/optics	-15 to 30 (5 to 86)	-15 to 35 (5 to 95)	0 to 30 (32 to 86)	-15 to 30 (5 to 86)	-15 to 35 (5 to 95)	0 to 30 (32 to 86)	35(95)
TV-B vidicon/optics[c]	-15 to 30 (5 to 86)	-15 to 35 (5 to 95)	0 to 30 (32 to 86)	-15 to 30 (5 to 86)	-15 to 35 (5 to 95)	0 to 30 (32 to 86)	35(95)
IRR	-30 to 30 (-22 to 86)	-30 to 30 (-22 to 86)	-20 to 0 (-4 to 32)	-30 to 35 (-22 to 95)	-30 to 35 (-22 to 95)	-30 to 30 (-22 to 86)	40(104)
UVS	-5 to 20 (23 to 68)	-5 to 20 (23 to 68)	0 to 20 (32 to 68)	-25 to 30 (-13 to 86)	-30 to 35 (-22 to 95)	-25 to 30 (-13 to 86)	40(104
Appendages							
Solar panels	-34 to 66 (-30 to 150)	-101 to 93 (-150 to 200)	-34 to 66 (-30 to 150)	-34 to 66 (-30 to 150)	-101 to 93 (-150 to 200)	-34 to 66 (-30 to 150)	66 (150)
Cruise sun sensor and gate	-29 to 43 (-20 to 110)	-30 to 55 (-22 to 131)	-12 to 49 (10 to 120)	-30 to 55 (-22 to 131)	-30 to 55 (-22 to 131)	-12 to 43 (10 to 110)	55 (131)
Acquisition sun sensor	-75 to 55 (-103 to 131)	-75 to 55 (-103 to 131)	-46 to 55 (-50 to 131)	-75 to 55 (-103 to 131)	-75 to 55 (-103 to 131)	-46 to 55 (-50 to 131)	55 (131)
A/C gas jet assemblies	-45 to 55 (-49 to 131)	-57 to 55 (-70 to 131)	-45 to 55 (-49 to 131)	-45 to 55 (-49 to 131)	-59 to 55 (-75 to 131)	-45 to 55 (-49 to 131)	55 (131)
Low-gain antenna and feed	-46 to 93 (-50 to 200)	-101 to 120 (-150 to 248)	-18 to 93 (0 to 200)	-46 to 93 (-50 to 200)	-101 to 120 (-150 to 248)	-18 to 93 (0 to 200)	66 (150)

Table 1 (contd)

Assembly	Operating range, °C(°F)			Nonoperating range, °C(°F)			Maximum acceptable temperature during ground operations (in air), °C(°F)
	Allowable long-term range (>1 h)	Allowable short-term range (<1 h)	Preferred range	Allowable long-term range (>1 h)	Allowable short-term range (<1 h)	Preferred range	
Medium-gain antenna and feed	-46 to 45 (-50 to 113)	-101 to 120 (-150 to 248)	-18 to 45 (0 to 113)	-46 to 45 (-50 to 113)	-101 to 120 (-150 to 248)	-18 to 45 (0 to 113)	66 (150)
High-gain antenna and feed	-35 to 93 (-31 to 200)	-101 to 120 (-150 to 248)	-18 to 93 (0 to 200)	-35 to 93 (-31 to 200)	-101 to 120 (-150 to 248)	-18 to 93 (0 to 200)	66 (150)
High-gain antenna deploy mech	-20 to 80 (-4 to 176)	-20 to 80 (-4 to 176)	-18 to 66 (0 to 150)	-20 to 80 (-4 to 176)	-20 to 80 (-4 to 176)	-18 to 66 (0 to 150)	55 (131)
Solar panel cruise dampers	-7 to 45 (19 to 113)	-7 to 45 (19 to 113)	-7 to 45 (19 to 113)	-20 to 45 (-4 to 113)	-20 to 45 (-4 to 113)	-7 to 45 (19 to 113)	55 (131)
Rocket engine[d]							
Bi-propellant valve	N/A	-7 to 66 (20 to 150)	N/A	-7 to 66 (20 to 150)	-7 to 121 (20 to 250)	21 to 38 (70 to 100)	41(105)
Injector head	N/A	-7 to 93 (20 to 200)	N/A	-7 to 71 (20 to 160)	-7 to 191 (20 to 375)	21 to 66 (70 to 150)	41(105)
Gimbal actuators	N/A	-7 to 135 (20 to 275)	N/A	-7 to 66 (20 to 150)	-7 to 135 (20 to 275)	21 to 66 (70 to 150)	66(150)
Gimbal bearings	N/A	-7 to 204 (20 to 400)	N/A	-7 to 71 (20 to 160)	-7 to 204 (20 to 400)	21 to 66 (70 to 150)	41(105)
Propulsion module[d]							
Pressurant tanks	N/A	-46 to 38 (-50 to 100)	N/A	-1 to 32 (30 to 90)	-46 to 38 (-50 to 100)	10 to 21 (50 to 70)	41 (105)
Pressurant control assembly	N/A	-18 to 38 (0 to 100)	N/A	-1 to 32 (30 to 90)	-18 to 38 (0 to 100)	10 to 21 (50 to 70)	41 (105)
Pressurant check-relief	N/A	-7 to 38 (20 to 100)	N/A	-1 to 32 (30 to 90)	-7 to 38 (20 to 100)	10 to 21 (50 to 70)	41 (105)
Propellant tank assemblies	N/A	-7 to 38 (20 to 100)	N/A	-1 to 32 (30 to 90)	-7 to 49 (20 to 120)	10 to 21 (50 to 70)	32 (90)
Maximum propellant tank gradient	N/A	N/A	N/A	(-1)30	N/A	6(10)	N/A
Propellant isolation assemblies	N/A	-7 to 49 (20 to 120)	N/A	-1 to 32 (30 to 90)	-7 to 66 (20 to 150)	10 to 21 (50 to 70)	41 (105)

Abbreviations: AC = altitude control; FCS = flight command subsystem; FTS = flight telemetry subsystem; RFS = radio frequency subsystem; DAS = data automation subsystem.

[a]TV electronics to be maintained within ±5°C(9°F) of nominal during orbital operations.

[b]IRIS optics temperature requirements are applicable to nominal conditions only. The allowable short and long term ranges may be exceeded during earth cruise (non-operating), Mars apoapsis (operating), and when the scan platform viewing direction is greater than ±10° from the local vertical (operating). The preferred and operating temperatures can be any value between -26°C (-14°F) and -21°C (-5°F) with a tolerance on that value of ±0.5°C (0.9°F) (thermostatic heater control dead-band). The preferred temperature is required during all data taking periods when the scan platform viewing direction is within ±10° of the local vertical.

[c]Maximum allowable operating axial gradient along the TV-B optics housing to be 5°C (9°F).

[d]Range time may be greater than 1-h due to soakback period of rocket engine and propulsion module.

Table 2. Spacecraft bus comparisons

	MM'64	MV'67	MM'69	MM'71
Louvered bays	6	6	5	6
Fully shielded bays	1	1	1	1
Unshielded bays	0	0	1	1
Midcourse motor bays	1	1	1	0
Earth cruise electronic power dissipation, W	132	142	201	167
Earth cruise average bus temperature, °C (°F)	21(70.5)	13(56)	22(71)	16(60)

Table 3. Comparison of test temperatures with analytical predictions

Location	Thermal control model, °C (°F)				Proof test model, °C (°F)			
	Cold mode		Hot mode		Earth cruise		Mars orbit	
	Predict	Actual	Predict	Actual	Predict	Actual	Predict	Actual
Bus								
Bay I average	16(60)	17(62)	25(77)	30(86)	18(65)	18(64)	21(69)	20(68)
Bay II	17(62)	18(64)	31(87)	36(96)	21(69)	19(66)	23(73)	21(69)
Bay III	17(62)	18(64)	34(93)	38(100)	21(70)	19(66)	24(76)	19(66)
Bay IV	22(71)	16(60)	38(101)	39(103)	25(77)	19(67)	29(85)	21(69)
Bay V	13(56)	10(50)	22(71)	29(85)	16(61)	14(57)	19(67)	19(67)
Bay VI	14(57)	13(56)	41(105)	58(118)	23(74)	16(60)	37(99)	27(81)
Bay VII	10(50)	4(39)	25(77)	35(95)	14(57)	9(49)	24(76)	21(70)
Bay VIII	8(47)	4(39)	20(68)	29(85)	20(68)	12(53)	24(76)	18(64)
Scan platform								
IRIS base	2(36)	-2(28)	10(50)	21(69)	6(43)	9(49)	18(65)	14(57)
TV-B camera	4(40)	5(41)	19(67)	23(74)	4(40)	8(47)	21(69)	13(55)
UVS optics	-6(21)	-3(26)	2(36)	11(51)	-3(27)	2(35)	16(60)	11(51)
TV-A camera	-2(28)	-2(29)	6(43)	20(68)	-3(27)	-3(26)	13(56)	2(36)
IRR	-16(3)	-18(-1)	-9(15)	2(36)	-16(3)	-11(13)	-3(27)	-4(25)
Cone actuator	6(43)	4(39)	16(61)	18(64)	3(38)	8(47)	17(62)	14(57)

Table 4. Test/analysis comparison summary

Absolute Difference °C (°F)	Numbers of measurements for given spacecraft and mode			
	Thermal control model		Proof test model	
	Cold	Hot	Earth cruise	Mars orbit
0 - 2.2(0-4)	8	2	5	4
2.8- 5.0(5-9)	3	4	6	4
5.6- 7.8(10-14)	3	2	3	3
8.3-10.5(15-19)	0	4	0	2
11.1-13.9(20-25)	0	2	0	1

Table 5. Test and flight temperatures, in °C (°F)

Location	Mars orbit			Earth cruise				Preferred operating range
	Phase II PTM test	M'71-1 test	M'71-2 test	Phase II PTM test	M'71-1 test	M'71-2 test	Mariner 9 (M'71-2 flight)	
Bus								
Bay I (power)	20 (68)	19 (66)	19 (67)	18 (64)	16 (61)	17 (62)	17 (63)	10 to 32 (50 to 90)
Bay II (power, IRIS, SCAN)	21 (69)	20 (68)	20 (68)	19 (66)	18 (65)	18 (65)	19 (66)	14 to 37 (58 to 98)
Bay III (CC&S, A/C)	19 (66)	18 (65)	18 (64)	19 (66)	18 (65)	18 (65)	18 (65)	18 to 35 (65 to 95)
Bay IV (FCS, FTS)	21 (69)	21 (69)	21 (69)	19 (67)	19 (67)	21 (69)	18 (64)	10 to 32 (50 to 90)
Bay V (DSS)	19 (67)	17 (63)	18 (65)	14 (57)	14 (57)	16 (60)	13 (56)	10 to 32 (50 to 90)
Bay VI (RFS)	22-42 (72-107)	23-48 (74-118)	24-48 (76-118)	14-23 (57-73)	15-28 (59-82)	16-27 (60-80)	14-24 (58-76)	10 to 32 (50 to 90)
Bay VII (DAS, TV)	21 (70)	21 (70)	20 (68)	9 (49)	10 (50)	9 (49)	9 (49)	10 to 32 (50 to 90)
VIII (Battery)	18 (64)	18 (64)	19 (66)	12 (53)	10 (50)	11 (52)	13 (55)	10 to 18 (50 to 65)
Propulsion module								
Rocket engine								
Bi-propellant valve	29 (85)	34 (93)	29 (85)	54 (129)	59 (139)	54 (130)	53 (128)	-7 to 66 (20 to 150)
Fuel tank	16 (61)	17 (63)	17 (62)	19 (66)	20 (68)	19 (67)	21 (69)	-1 to 32 (30 to 90)
Oxidizer tank	16 (60)	17 (63)	16 (61)	18 (65)	19 (66)	18 (65)	19 (67)	-1 to 32 (30 to 90)

Table 5 (contd)

Location	Mars orbit			Earth cruise				Preferred operating range
	Phase II PTM test	M'71-1 test	M'71-2 test	Phase II PTM test	M'71-1 test	M'71-2 test	Mariner 9 (M'71-2 flight)	
Scan platform								
IRR	-3 (27)	1 (34)	2 (35)	-8 (18)	-4 (24)	-4 (25)	-7 (20)	-20 to 0 (-4 to 32)
TV-A	6 (42)	13 (55)	12 (53)	2 (36)	8 (46)	8 (46)	6 (42)	10 to 16 (50 to 60)
UVS	11 (51)	16 (60)	11 (51)	3 (37)	6 (42)	4 (39)	3 (37)	0 to 20 (32 to 68)
TV-B	13 (56)	16 (60)	14 (57)	10 (50)	12 (53)	12 (53)	8 (47)	10 to 16 (50 to 60)
IRIS base	14 (57)	11 (51)	10 (50)	10 (50)	8 (46)	9 (48)	---	-3 to 27 (27 to 80)

Table 6. Temperature control subsystem equipment list

Item	Mass, kg (lb_m)	
	kg	lb
Upper thermal blanket assembly	5.08	(11.2)
Lower thermal blanket assembly	0.64	(1.4)
Planetary platform thermal blanket assembly	0.95	(2.1)
Planetary platform louver assembly	0.45	(1.0)
Platform louver assembly support bracket	0.54	(1.2)
Bay louver assemblies (6, at 0.62 kg each)	3.72	(8.2)
Rocket engine thermal shield assembly	0.32	(0.7)
Rocket engine thermal blanket	0.09	(0.2)
Lower bay channel shields (7)	0.09	(0.2)
Corner shields (8)	0.41	(0.9)
Full shield, Bay IV	0.23	(0.5)
Miscellaneous small shields and shades	0.09	(0.2)
Miscellaneous attachment hardware	0.64	(1.4)
Total	13.3	(29.2)

Table 7. Results of propulsion module effective emittance tests

Mode No.	Blanket configuration[a] Inner to outer layer →								Power, W	Average temperature, °C (°F)	Effective emittance, ϵ_{eff}	Weight, kg (lb)
	D	10	5a	5b	69	A	M	Other				
1	X	X				X			18.15	21 (70.6)	0.0004	3.9 (8.6)
2	X	X				X	X		15.15	22 (71.0)	0.0054	
3	X	X	X			X			16.1	22 (72.0)	0.0056	4.6 (10.2)
4	X	X	X	X		X			13.6	23 (72.6)	0.0048	5.4 (11.8)
5	X		X	X		X			18.8	21 (70.5)	0.0067	4.0 (8.7)
6	X		X			X			23.1	22 (70.8)	0.0083	3.2 (7.0)
7	X				X	X			17.5	22 (71.2)	0.0062	4.3 (9.4)
8	X	X	X			X		b	18.4	22 (70.9)	0.0066	
9	X	X	X			X		b	15.3	4 (38.9)	0.0069	

[a]Definition of blanket configuration symbols:

D Dacron slipcover. A single-layer blanket made of Dacron cloth to serve as a removable inner layer.

10 Ten-layer blanket. Ten layers of 0.0038-mm (1/8-mil) Mylar, aluminized on both sides, alternated with ten layers of Nylon net (Mariner Mars 1971 net) so that the blanket has a Mylar inner layer and a net outer layer.

5a and 5b Five-layer blankets. Each made up of five layers of 0.0038-mm (1/8-mil) Mylar, aluminized on both sides, alternated with five layers of Nylon net (Mariner Mars 1971 net) so that each blanket has a Mylar inner layer and a net outer layer.

69 Blanket constructed with Mariner Mars 1969 materials and techniques, made up of ten layers of 0.0063-mm (1/4-mil) Mylar, aluminized on both sides, alternated with 10 layers of Nylon net (Mariner Mars 1969 net) so that the blanket has a Mylar inner layer and a net outer layer.

A Armalon slipcover. A single-layer blanket made of Armalon (Beta cloth) to serve as a removable outer layer.

M Low-emittance Mylar slipcover. A single-layer blanket made of 0.0127-mm (1/2-mil) Mylar, aluminized on both sides, to serve as a removable outer layer.

[b]Flightlike blanket with engine and omnicutouts covered with 0.051-mm (2-mil) aluminized Kapton, aluminum side out.

Table 8. Mariner 9 earth cruise temperatures: Day 155 GMT, 16:00

Measurement		Temperature, °C (°F)		
Channel	Name	M'71-2 predicts	M'71-2 actuals	Difference
E404	VCO	16 (60)	16 (60)	0
E405	Battery	11 (51)	13 (55)	+2 (+4)
E407	Canopus sensor	12 (53)	12 (53)	0
E408	Oxidizer tank	22 (71)	19 (67)	-2 (-4)
E409	Fuel tank	23 (73)	21 (69)	-2 (-4)
E410	IRR	-6 (22)	-7 (20)	-1 (-2)
E430	Auxiliary oscillator	16 (60)	17 (62)	+1 (+2)
E411	Bay I	16 (61)	17 (63)	+1 (+2)
E431	Prop N_2 tank	18 (64)	16 (61)	-2 (-3)
E412	Bay III	18 (64)	18 (65)	+1 (+1)
E432	Bay IV	20 (68)	18 (64)	-2 (-4)
E413	Bay V	15 (59)	13 (56)	-2 (-3)
E433	TWT No. 2 base	14 (58)	24 (76)	+10 (+18)
E414	Bay VII	9 (48)	9 (49)	+1 (+1)
E434	Bay II	18 (64)	19 (66)	+1 (+2)
E415	TV-A vidicon	6 (42)	6 (42)	0
E435	TV-B vidicon	9 (49)	8 (47)	-1 (-2)
E416	UVS detector	3 (38)	3 (37)	-1 (-1)
E436	TV-B optics	7 (44)	6 (43)	-1 (-1)
E417	Sun sensor	44 (112)	49 (120.5)	+5 (+8)
E437	IRIS optics	-24 (-12)	-24 (-12)	0
E418	TWT No. 1 base	28 (82)	14 (58)	14 (-24)
E438	+X/-Y N_2	13 (56)	13 (56)	0
E419	+Y Solar panel	52 (125)	50 (122)	-2 (-3)
E439	Engine injector	59 (139)	60 (140)	+1 (+1)
E215	Engine valve	54 (129)	53 (128)	-1 (-1)
E219	Engine thermal blanket	68 (154)	69 (156)	+1 (+2)

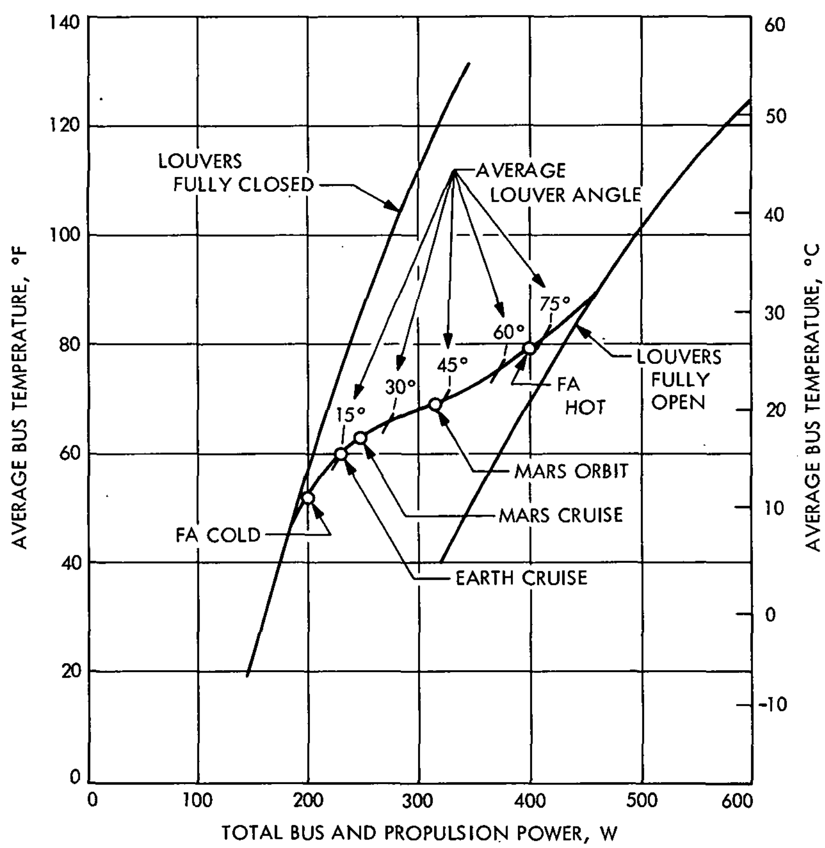

Fig. 1. Average bus temperature vs power

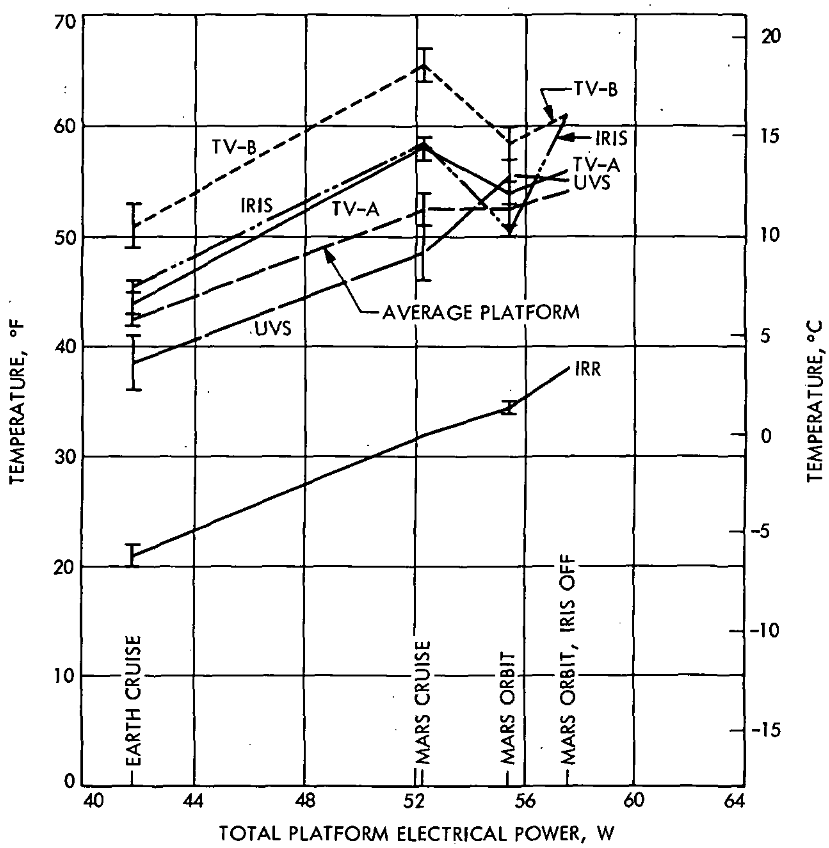

Fig. 2. Scan platform temperature distribution

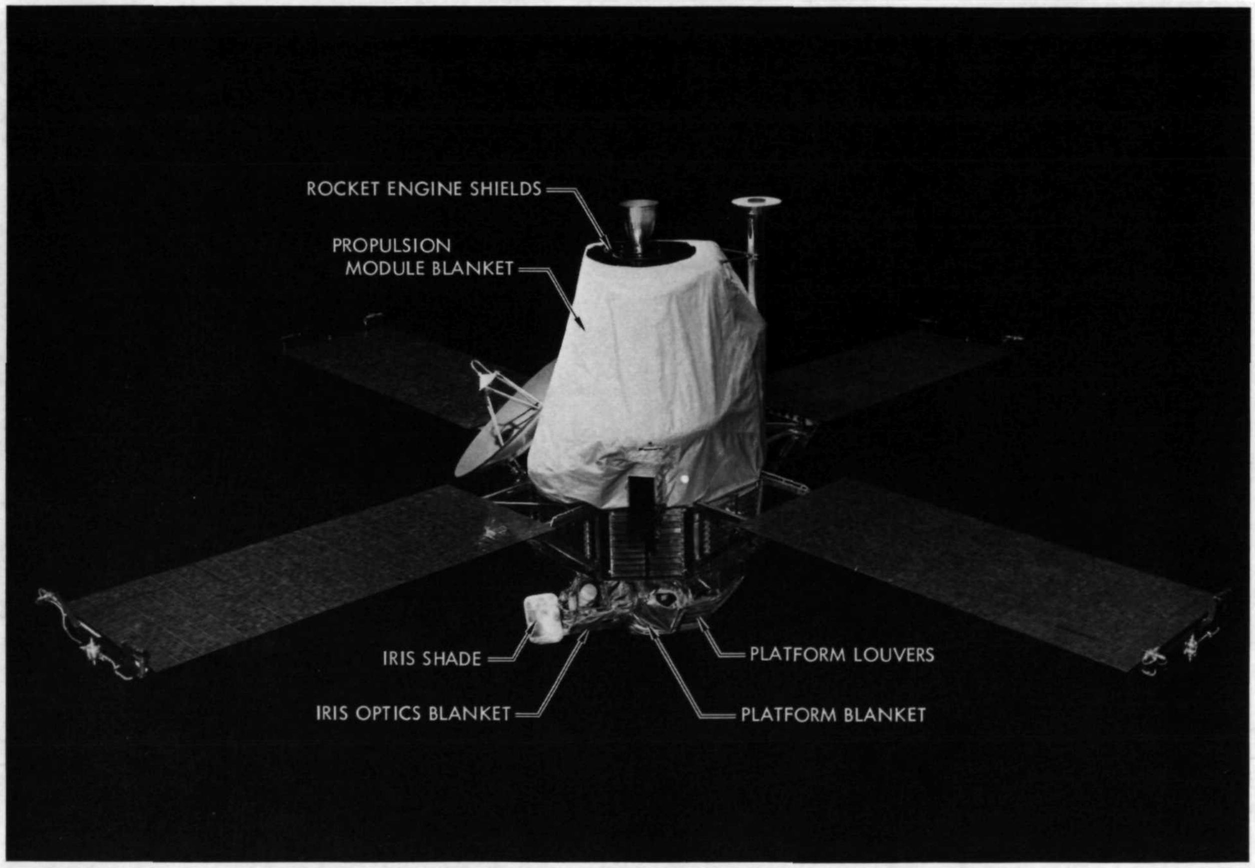

Fig. 3. Mariner Mars 1971 spacecraft, top view, Bay VIII side

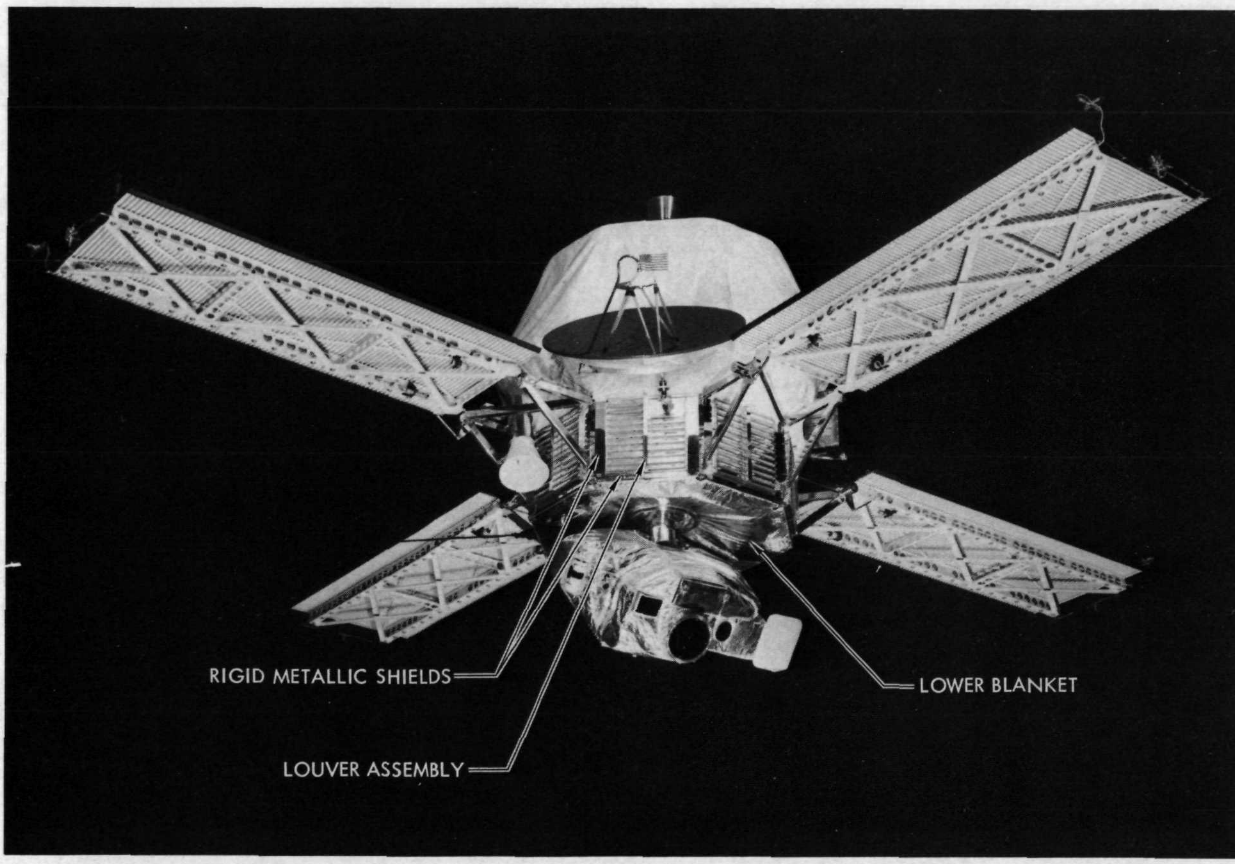

Fig. 4. Mariner Mars 1971 spacecraft, bottom view, Bay II side

Fig. 5. Propulsion module mold

NASA — JPL — Coml., L.A., Calif.